Flexible and Printed Electronics

OPEN ACCESS

RECEIVED
16 January 2024

REVISED
19 March 2024

ACCEPTED FOR PUBLICATION
26 April 2024

PUBLISHED
15 May 2024

PAPER

Inkjet-printed heater on flexible substrates for low voltage applications

Muhammad Atif Khan, Danial Khan and Yehia Massoud*

Innovative Technologies Laboratories (ITL), King Abdullah University of Science and Technology (KAUST), Riyadh, Saudi Arabia
* Author to whom any correspondence should be addressed.

E-mail: yehia.massoud@kaust.edu.sa

Keywords: flexible heater, printed heater, inkjet printing, resistive heating

Supplementary material for this article is available online

Abstract

Flexible heaters (FHs) have applications ranging from defoggers to flexural warmers, food processors, and thermotherapy. Printed FHs are particularly of interest as they offer unique advantages like high resolution, customization, low cost, and ease of fabrication. Here, we report printed FHs on polyethylene terephthalate substrate. The heater design is optimized to operate on a low voltage of five volts and yield high temperatures with a uniform temperature distribution across the surface. The heater has a fast response time of 15 s to reach its maximum temperature and does not show any degradation in performance after three months of operation. The heater maintains its temperature after continuous use for two hours and exhibits a minimum change in temperature upon bending. We have also developed and tested designs for zone heaters and nano heaters, where zone heater is suited for applications requiring heating in specified locations on a surface only. Whereas nano heater has an area of 1 mm^2 and can produce high temperatures in this small area. Finally, we developed similar printed heaters on paper and polyimide (PI) substrates as well. Paper-based heater can achieve a temperature of 210 °C and can be used in disposable applications due to its low cost, whereas PI heater can achieve a temperature of 380 °C and is suitable for attaining high temperatures. These results manifest the use of FHs for various practical applications.

1. Introduction

During the past few decades, the outlook of electronics is transitioning from rigid and brittle to flexible and bendable [1]. The flexible electronics possess several advantages like lightweight, low cost, and easy to manufacture [1, 2]. Due to these advantages, flexible devices have tremendous potential in applications like wearables, displays, energy harvesting, and entertainment gadgets [1, 2]. Likewise, traditional electrothermal heaters are heavy, rigid, and bulky and can be used for limited applications only. Recently, flexible heaters (FHs) have been enormously researched. Contrary to their traditional counterparts, FHs are directly used in several applications. For example, FHs are used for defogging and deicing in automobiles and windows [3, 4]. Some outdoor devices and sensors cannot operate properly in extreme weather conditions, FHs are used as flexural warmers to maintain the temperature and ensure the proper operation of the device [5]. Other applications include warming garments, thermotherapy through wearables, food processing, portable devices, and drug delivery [6–11].

FHs work on the principle of Joule heating where the electrical energy of the electric current is converted to the heat energy. Mostly a conductive path is created on a flexible substrate for the electric current to flow and dissipate energy to increase the temperature. Previously, FHs were mostly fabricated using different types of coating techniques like spin coating, bar coating, spray coating, and dip coating [12–14]. However, coating techniques have limited resolution and have a high cost associated with them. With the advancement of printing techniques, it has become the most widely used method for preparing the FHs. Different printing techniques like inkjet printing, screen printing, and gravure printing have been explored for the preparation of FHs [13, 15]. Among these techniques, inkjet printing offers high resolution, freedom in customized printing, facile fabrication, and low cost. Using inkjet printing, desired patterns can be fabricated directly with a resolution of mm scale. The inkjet printing of FHs is a relatively new and developing technique and therefore there are very few reports of inkjet-printed FHs. Byers *et al* reported a low-power thermal heater [16]. Mitra *et al* reported silver ink-based FHs on polyethylene naphthalene substrate [17]. Hu *et al* reported electrohydrodynamic printing using composite ink for the preparation of FHs [18]. Wang *et al* and Huang *et al* reported silver nanowire-based flexible and stretchable heaters [19, 20].

The figures of merit of a FH are low operating voltage, fast heating and cooling, broad heating range, uniform temperature distribution, and long-term thermal stability [12]. Considering these parameters, here we report FHs on various flexible substrates like polyethylene terephthalate (PET), paper, and polyimide (PI) substrate. We started by testing the conductivity of the ink and then optimizing the design to generate a temperature of 100 °C at an applied voltage of 5 V. The design was further optimized to obtain a uniform distribution of temperature. The time to reach a stable temperature was measured by monitoring the current of the heater. We further analyzed the operation of the FH under strain by fully bending the FH. Next, we demonstrated some applications of FH by illustrating the working of a zone heater and a nano heater. A zone heater provides heating in a specific area only to obtain a temperature gradient. The nano heater has a heating area of 1 mm^2 and is suited for applications where heating is required in a confined area only. Finally, we fabricated FHs on paper and PI substrate. On a PET substrate, the maximum achievable temperature is 120 °C limited by the melting of PET. On paper and PI substrates, temperatures up to 210 °C and 380 °C can be conveniently achieved, respectively.

2. Experimental section

The fabrication of the FHs started from designing the FHs. The FHs were designed in the computer simulation technology studio and the Gerber file was extracted from the design. Then the FHs were printed on flexible substrates using a Voltera Vone inkjet printer (shown in figure S1 in supplementary information). The ink used for the printing was Conductor-III ink from Voltera. After printing, the ink was dried by heating at 120 °C for 20 min. PET and PI sheets were also purchased from Voltera.

The infrared images were taken using the Hti Thermal Imaging Camera. The electrical measurements were performed by the Keithley DC power supply (shown in figure S2 in supplementary information). The FH was kept suspended during measurement to minimize the effects of surroundings.

3. Results and discussion

We started by measuring the electric resistance of the conductive ink. Conductive ink III is used for printing the FH on a PET substrate. We printed the design shown in figure 1(a) and measured the electrical resistance of the ink. The length and width of each line shown in figure 1(a) are 50 mm and 1 mm, respectively.

Instead of a straight line, this design was selected because the maximum print area of the Voltera Vone printer is 128 mm × 112 mm. The electrical resistance of the ink is shown in figure 1(b). The resistance increases linearly with the length of the design and varies from ∼1 Ω to ∼4 Ω when the length increases from 50 mm to 200 mm. By taking advantage of the printed circuit, we prepared another device with the same design except that in this new device, the same design is printed on the PET substrate twice. This was done by first printing the design on PET and after letting it dry, printing the same design on top of it with the same ink. This increased the height of the ink and resulted in a reduction of device resistance as shown in figure 1(b). In this device, the resistance also increases linearly with length, but the total resistance of 200 mm length is less than 1 Ω. Using a similar approach, another device with three layers of ink was printed. Using the third layer of ink did not make a substantial change in the device resistance. Only a slight difference in the total resistance of the second and third devices was observed as seen in figure 1(b). Next, we applied a voltage across the first and second devices and measured their temperature profiles using an Infrared camera as exhibited in figures 1(c) and (d). For the first device, the temperature distribution across the device is not uniform. This inhomogeneity in the temperature distribution can be attributed to the nonuniform resistance distribution across the device. Since the same current flows through the entire device, the areas in the device with high resistance attain high temperatures due to Joule heating whereas the areas with low resistance maintain a low temperature. For the operation of a heater, the temperature across the entire device must be uniform. The resistance distribution in the second device is uniform due to two layers of ink printing and therefore the temperature uniformity was achieved in the second device as shown in figure 1(d). Since two layers of printing can offer a low resistance as well as uniform resistance distribution in the device, from here

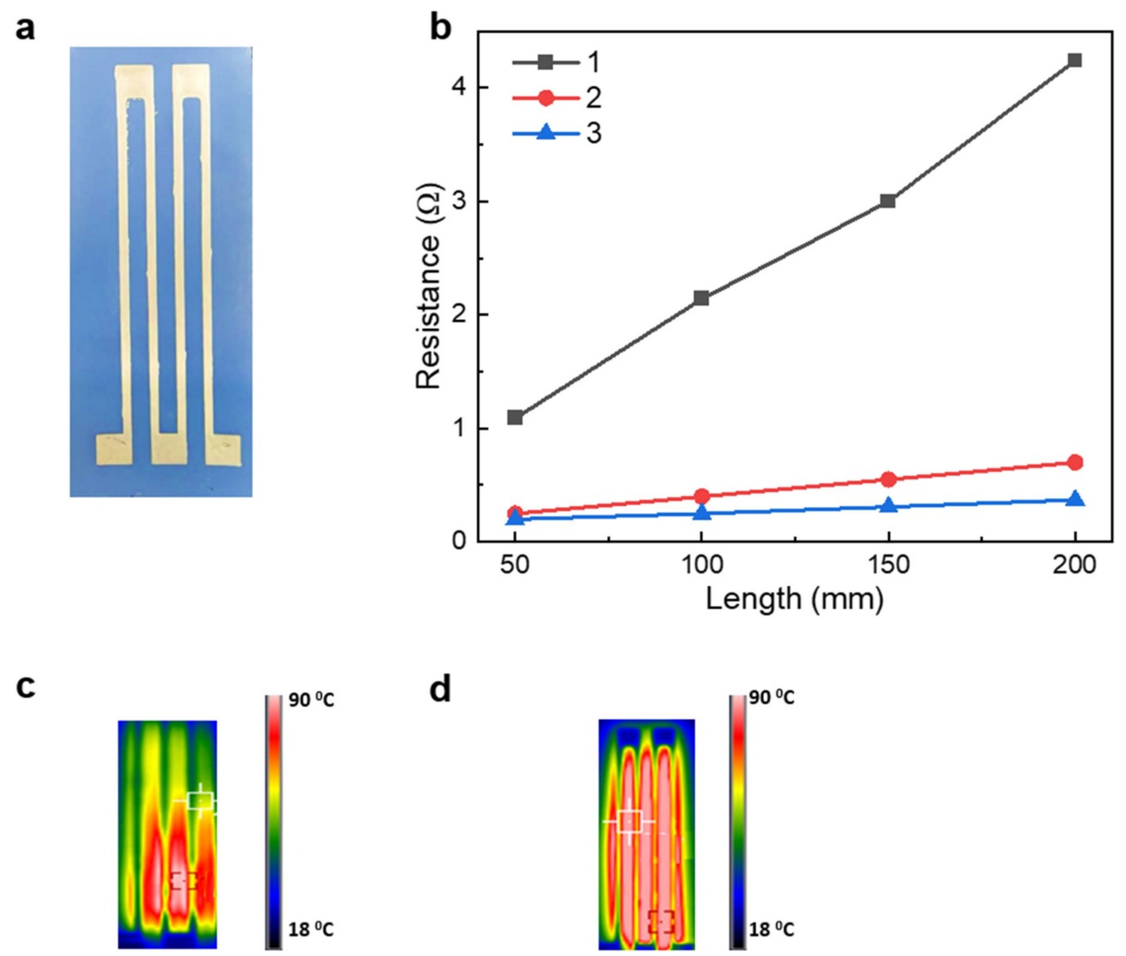

Figure 1. (a) Picture of the design used to measure the electrical resistance of the ink. (b) The electric resistance of the ink as a function of the length of the line for single, double, and triple-printed designs. (c) Infrared image of single printed design under applied voltage. (d) Infrared image of single printed design under applied voltage.

onwards all the devices discussed in the paper were prepared by printing two layers of the conductive ink.

After optimizing the printing conditions, we studied the effect of line width on the device resistance as well as the heating temperature. For this purpose, we prepared two devices with the same area and different line widths i.e. 0.5 mm and 1 mm as shown in figure 2. Figure 2(c) illustrates that the resistance of the device increases as the length of the line increases. On the contrary, the resistance decreases as the width of the line increases. The resistance of the device with the 0.5 mm line width remains half of the other device for all the lengths of the line. We also studied the effect of line width on the temperature of the devices under applied voltage as shown in figure 2(d). We found that the maximum achievable temperature is limited by the melting temperature of the substrate i.e. 120 °C.

Further, the device with low resistance can attain higher temperatures at a lower voltage since it carries a higher current at the same voltage. For example, at 3 V, the 0.5 mm device has a temperature of 64 °C and the 1 mm device has a temperature of 96 °C.

Next, we emphasize preparing a device that can produce a temperature of 100 °C at an applied voltage of 5 V. For this purpose, we prepared the devices presented in figure 3. These devices can attain a temperature close to 100 °C at an applied voltage of 5 V. We selected 100 °C because it is a sufficiently high temperature for most applications utilizing FH like defoggers, etc. Similarly, 5 V is a commonly used available voltage in most applications and can be obtained from batteries or power supplies. In the presented three devices, the length of each line is 40 mm, and the width of the line is 0.4 mm, and the resistance of each device is close to 8.5 Ω. The distance between the lines is 1.5 mm, 3 mm, and 4.5 mm in figures 3(a)–(c) respectively. The IR images taken from each device under the application of voltage illustrate that the temperature across the entire surface is uniform in figure 3(a). For figures 3(b) and (c), as the distance between the lines increases, the temperature distribution becomes non-uniform. The temperature in the gap between the lines is lower than the line temperature. The trade-off in the selection of the designs is between the large area coverage and the uniformity of the temperature. For example, the first design is best suited for applications that require a strictly uniform distribution.

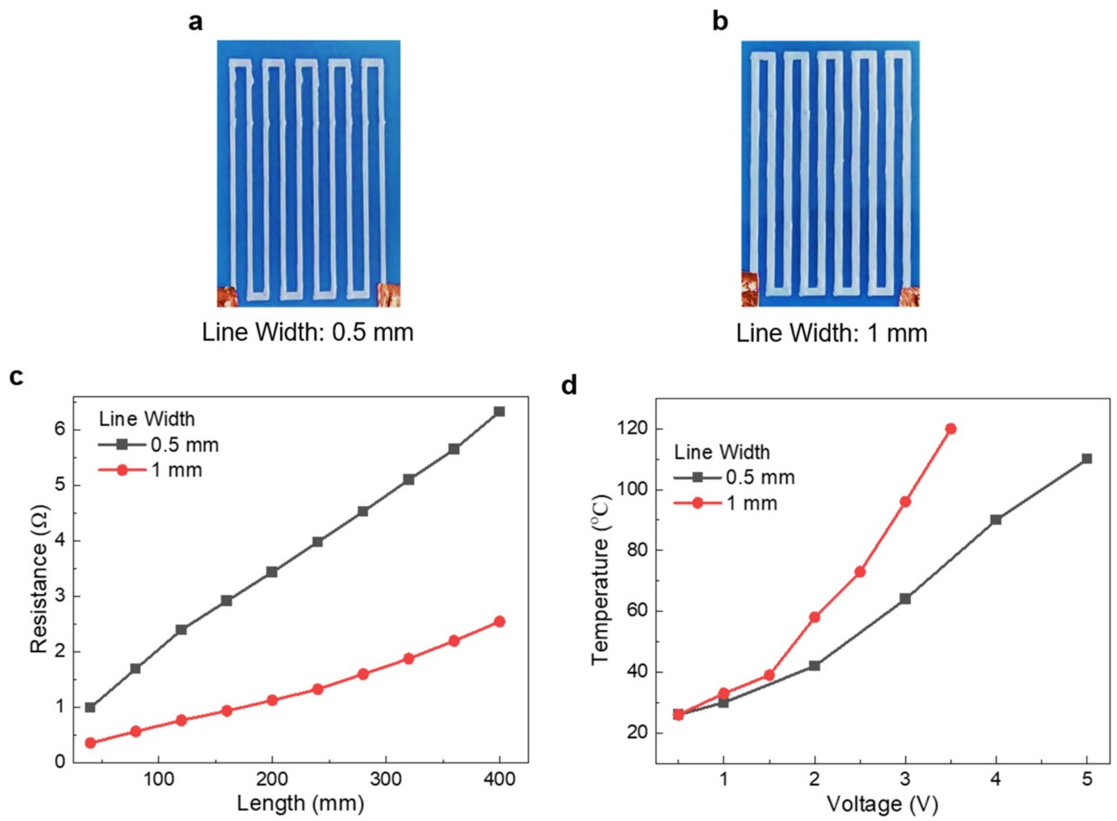

Figure 2. (a) Picture of the device with 0.5 mm line width. (b) Picture of the device with 1 mm line width. (c) Length versus resistance of the device for different line widths. (d) Voltage versus temperature of the device for different line widths.

From here onwards, we shall further analyze the first design only. Figure 3(d) presents the temperature of the first device as a function of applied voltage. A temperature of 100 °C is achieved at an applied voltage of 5 V whereas the maximum voltage that can be applied to the device is 6 V. At this voltage, the device temperature reaches 120 °C, increasing the temperature beyond this would cause the PET substrate to melt and consequently, irreversible damage to the device may occur. The device in figure 3(a) has a dimension of 40 mm × 17.5 mm, to cover a large area, a series or parallel combination of such devices can be used. In the series combination, the applied voltage should increase proportionally to the number of devices in the series. Whereas, in the parallel combination same voltage can be applied to all the devices in parallel. We have illustrated the connection of three devices in series as well as parallel in figure S3 in the supplementary information.

Further characterization of the device presented in figure 3(a) has been illustrated in figure 4. The IR temperature profile of the device at the applied voltage of 6 V is shown in figure 3(b). It can be seen that the device's temperature is around 120 °C. When a voltage is applied, the peak current flows through the device, and then it gradually starts reducing and finally, it reaches a steady state value. This can be explained by the fact that the resistance of the ink starts to increase due to an increase in temperature when the current starts flowing. This causes a reduction in the device's current with time as the device's temperature increases with time. Finally, a steady state point is reached where the device temperature becomes constant, and a constant current starts to flow through it. Figure 4(c) illustrates that the time to reach the steady state temperature of 120 °C is around 15 s. This time is sufficiently fast enough to be used in various FH applications. After reaching the stable temperature, we ran the FH continuously for two hours and the FH maintained a stable temperature for two hours. The degradation of the FH over time was also studied and it was observed that FH exhibited negligible change in its performance even after three months. We also measured the starting current of the device as a function of applied voltage as illustrated in figure 3(d) and a linear relation has been observed between the current and voltage of the device.

Next, we explore FH in some other configurations. Figures 5(a) and (b) describe the bending test of our FH device. The device was fully bent as shown in figure 5(a) and no cracks or damages in the ink or substrates are observed even after bending multiple times. A 2% change in the device's resistance was observed after bending and twisting multiple times. Also as shown in figure 5(b), the device can attain

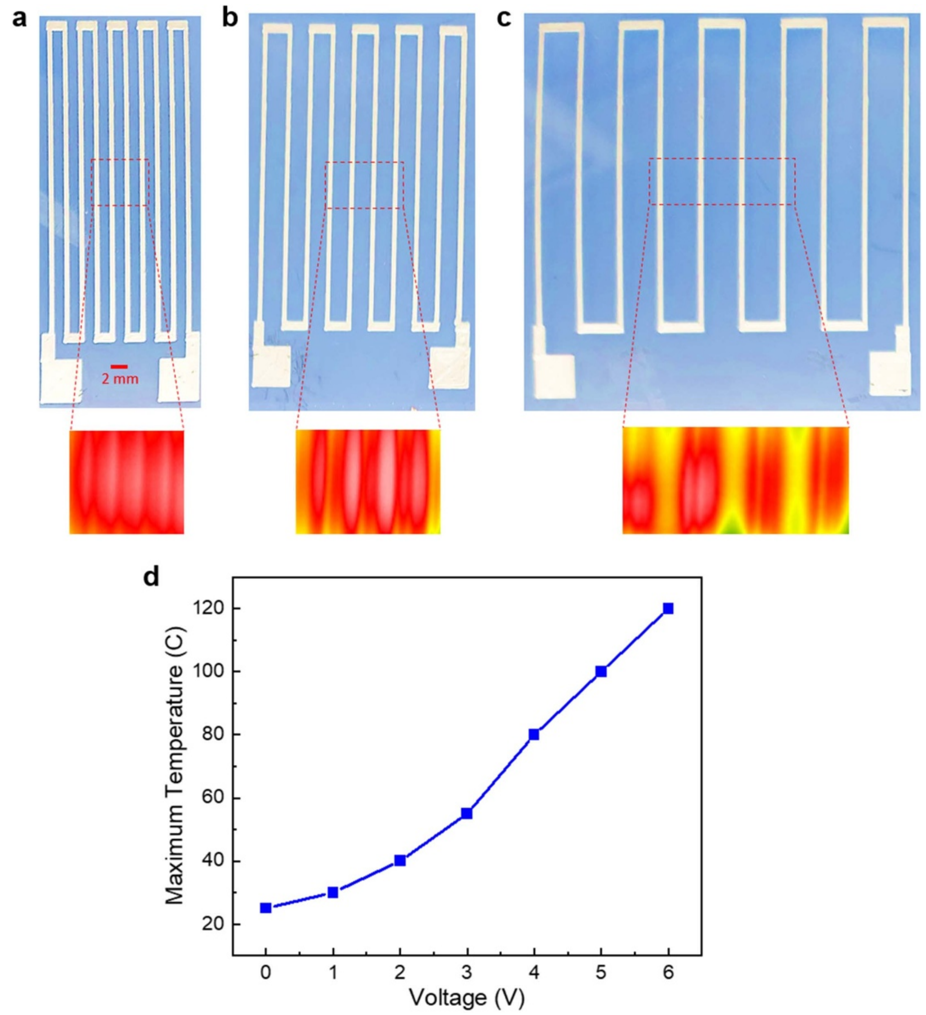

Figure 3. (a) Picture of the device with 1.5 mm spacing between the lines. The length of each line is 40 mm, and the width is 0.4 mm. (b) Picture of the device with 3 mm spacing between the lines. (c) Picture of the device with 3 mm spacing between the lines. (d) The maximum temperature of the device as a function of applied voltage.

similar temperatures in the bent position with slight change in temperature distribution across the surface. These advantages manifest the use of our FH for various applications including wearables and mountables. Since the device is printable, therefore any customized design can be made of this. As an example, we have demonstrated in figures 5(c) and (d), a device that has zones of heating and no heating. Such a device can be used for applications where high temperature is not required throughout the surface but in specified areas only. Here we have prepared three zones of 10 × 10 mm where the resistance of the line is high and therefore upon application of voltage, the temperature of this area increases. The width of the line is 0.3 mm in the high resistance areas and can be further tailored according to the requirements of the application. The resistance of the device is 10.95 Ω and the maximum temperature difference between the high-temperature and low-temperature areas is 90 °C. We also printed a nano heater with an area of 1 mm^2 and a resistance of 0.33 Ω. This heater can attain a high temperature of around 120 °C in a very small area. From figure 5(d), it can be seen that the heat is not confined to the area of the nano heater only but slightly spreads out. The area of the heater is 1 mm^2 but the heat spreads out to an area of 4 mm^2 as measured in our experiment.

Finally, to illustrate the diversity of our proposed FH, we prepared our FH on different flexible substrates. Figures 6(a) and (b) present the FH on a paper substrate. The maximum temperature attainable using paper substrate is limited by the ignition temperature of the paper as the paper does not melt at high temperatures. The ignition temperature of the paper is around 230 °C and therefore, on the paper substrate we have conveniently achieved a temperature of 210 °C using our FH. The paper substrate offers advantages like low cost, high temperature, and extreme flexibility and can be used for disposable and one-time use applications where durability is not of

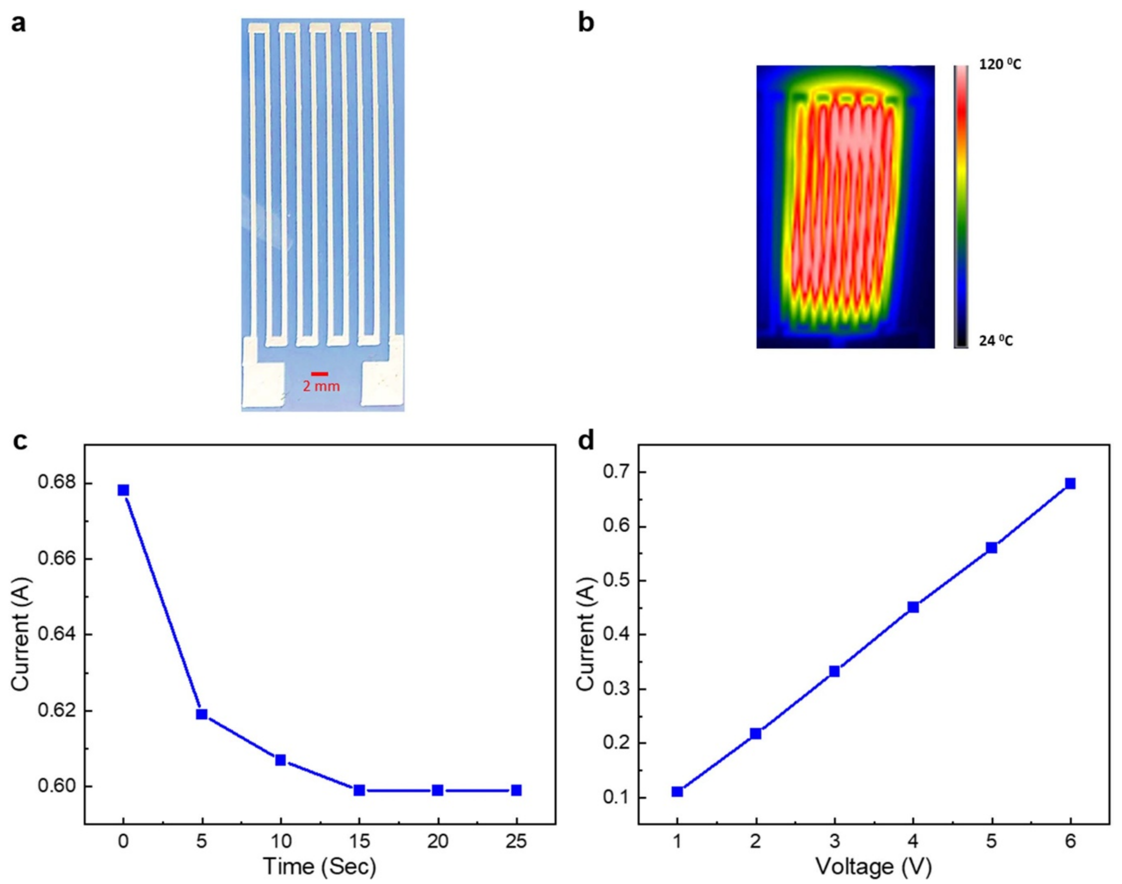

Figure 4. (a) Picture of the device with 1.5 mm spacing between the lines. (b) Infrared image of the device in (a) under application of 6 V bias. (c) The current of the device in (a) as a function of time. (d) The starting current of the device in (a) as a function of applied voltage.

concern. Next, we printed the same design on a PI substrate as shown in figure 6(c). The melting point of PI is close to 400 °C and we tested our design for 380 °C. PI is a commercially used substrate for printed electronics and flexible electrical components and can be used for applications where high-temperature heating is required. It is worth noting that the maximum heating temperature is not limited by the ink used for printing but rather by the melting or ignition temperature of the substrate. The voltage versus temperature graph for the PI device is shown in figure 6(e). The device can attain a temperature of 380 °C at an applied voltage of 6 V. Lastly, we demonstrated two applications of FHs as shown in figures 6(e) and (f) firstly, a PET-based FH is wrapped around a glass beaker to provide the heating. Such assembly can be used for deicing and defogging applications as well as warmers for outdoor sensors and appliances. Due to the flexible nature of FH, it can be conveniently wrapped around appliances for heating purposes.

Cold weather and infections of the upper respiratory tract (nose and throat) are often associated. A recent study has shown that the major reason behind such infections is that cold weather impairs our immune system against viruses and therefore we are more likely to catch an infection during cold weather [21]. In the second application shown in figure 6(f), we fitted a paper-based FH in a mask to modulate the temperature of the nose and mouth in cold weather. Since the nose and mouth are the first points of contact with infection-causing species like viruses or bacteria, using FH-fitted masks can boost immunity and protect against infections. Similar FHs can be fitted in gloves or other clothing items to serve as warming garments in harsh weather conditions.

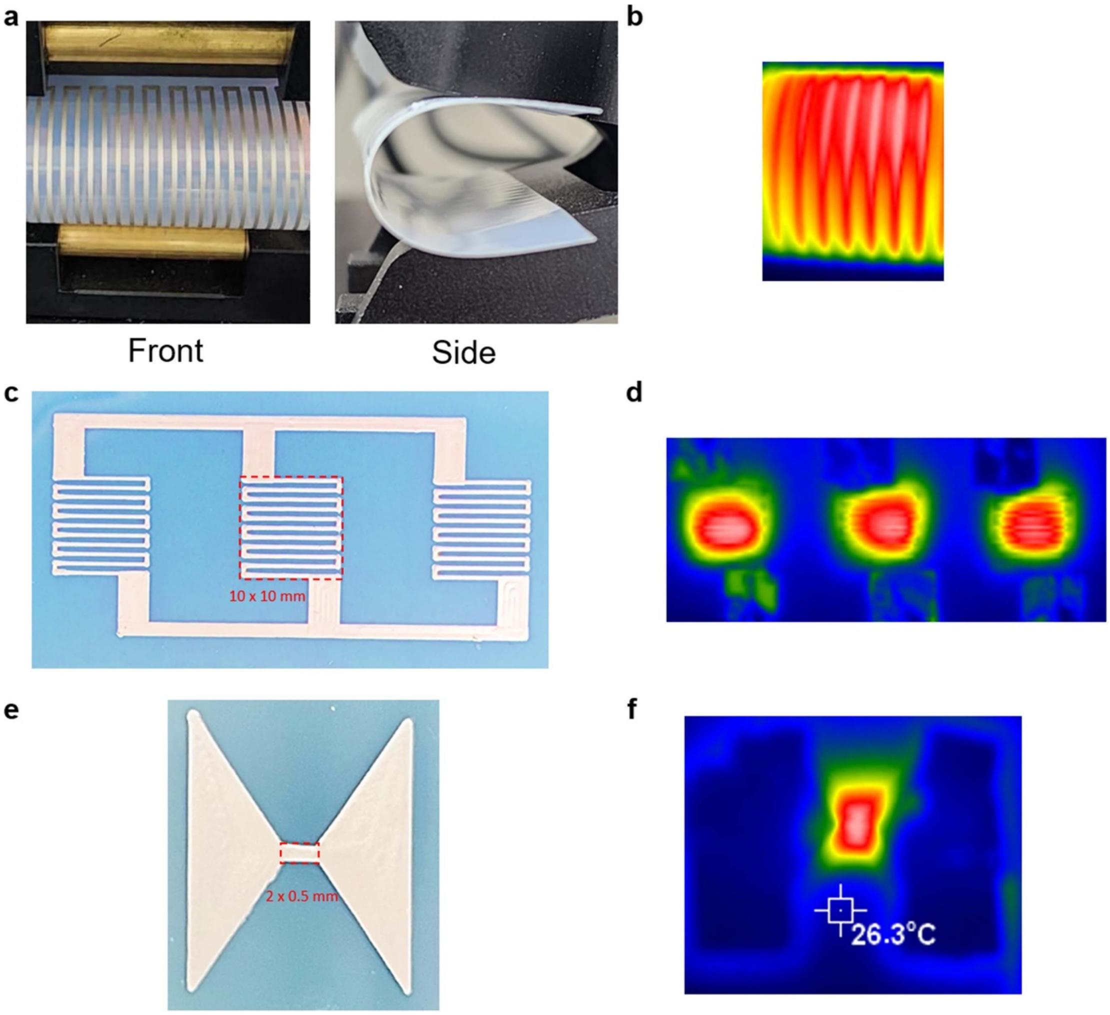

Figure 5. (a) The pictures illustrating the bending of the flexible heater from front and side. (b) Infrared image of the flexible heater taken during bending. (c) Zone heater with specialized zones for heating. (d) Infrared image of the zone heater taken during the applied bias. (e) Nano heater with a heating area of 1 mm^2. (f) Infrared image of the nano heater taken during the applied bias.

4. Conclusions

The operation and working of printed FHs on three flexible substrates have been demonstrated. The maximum achievable temperatures on PET, paper, and PI were 120 °C, 210 °C, and 380 °C, respectively. The maximum temperature is not limited by the conductive ink used for printing but rather by the melting/ignition temperatures of the substrates. The paper substrate offers a low price and can be a convenient option for disposable and one-time-use applications. The PET and PI substrates offer reliability and minimum degradation in performance upon bending and continuous use. We have tested by fully bending the FH, continuous use for two hours, and long-term use for three months with minimum degradation in the performance. FHs offer uniform temperature distribution across the surface with a fast response time of 15 s. Along with these advantages, the facile fabrication process of printed FHs makes them suitable for use in various practical applications.

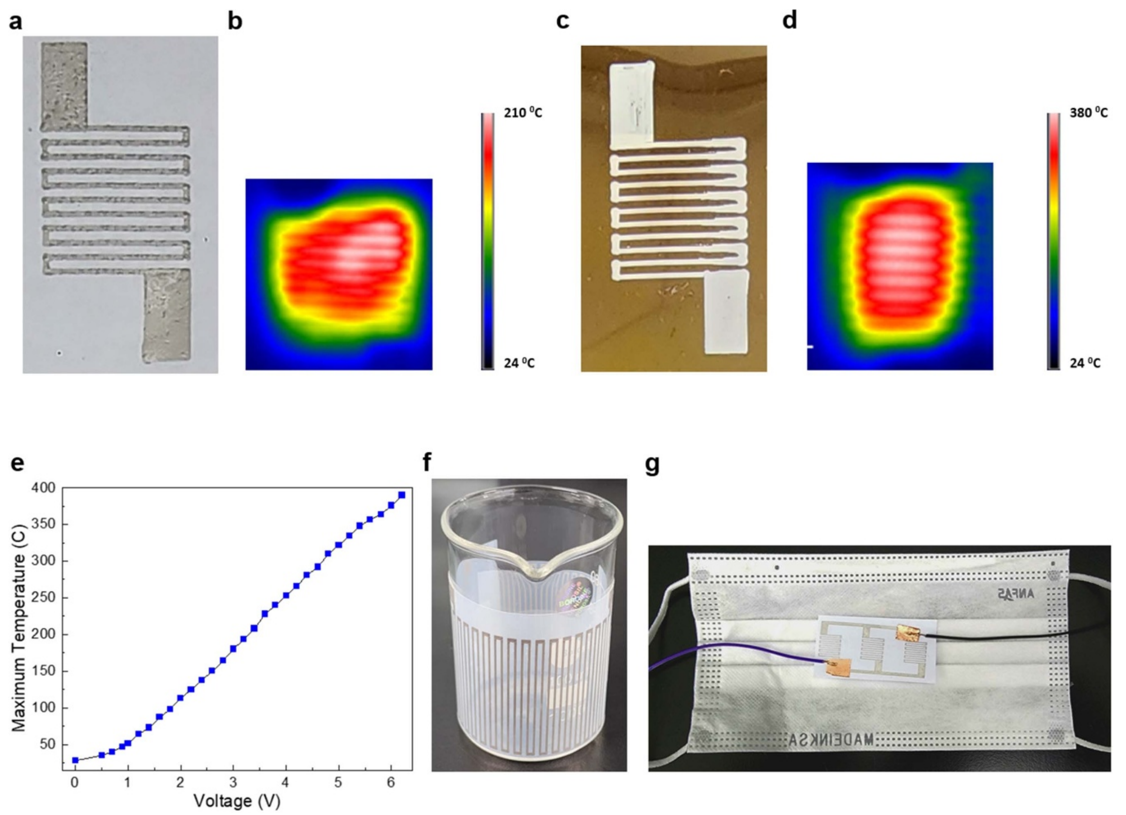

Figure 6. (a) Flexible heater printed on paper. (b) Infrared image of the flexible heater in (a) taken during the application of voltage. (c) Flexible heater printed on a polyimide substrate. (d) Infrared image of the flexible heater in (c) taken during the application of voltage. (e) Voltage versus temperature graph of PI device. (f) Flexible heater wrapped around a glass beaker for heating/defogging. (g) Flexible heater fitted inside a mask for heating purposes.

Data availability statement

The data cannot be made publicly available upon publication because they are not available in a format that is sufficiently accessible or reusable by other researchers. The data that support the findings of this study are available upon reasonable request from the authors.

ORCID iD

Danial Khan https://orcid.org/0000-0003-4010-2637

References

[1] Wong W S and Salleo A (eds) 2009 *Flexible Electronics: Materials and Applications* vol 11 (Springer Science & Business Media)

[2] Cheng I-C and Wagner S 2009 Overview of flexible electronics technology *Flexible Electronics: Materials and Applications* pp 1–28

[3] Kang T-W, Kim S H, Kim C H, Lee S-M, Kim H-K, Park J S, Lee J H, Yang Y S and Lee S-J 2017 Flexible polymer/metal/polymer and polymer/metal/inorganic trilayer transparent conducting thin film heaters with highly hydrophobic surface *ACS Appl. Mater. Interfaces* **9** 33129–36

[4] Jo H S, An S, Lee J-G, Park H G, Al-Deyab S S, Yarin A L and Yoon S S 2017 Highly flexible, stretchable, patternable, transparent copper fiber heater on a complex 3D surface *NPG Asia Mater.* **9** e347

[5] Hong S, Lee H, Lee J, Kwon J, Han S, Suh Y D, Cho H, Shin J, Yeo J and Ko S H 2015 Highly stretchable and transparent metal nanowire heater for wearable electronics applications *Adv. Mater.* **27** 4744–51

[6] Zhang H *et al* 2022 Bifunctional flexible electrochromic energy storage devices based on silver nanowire flexible transparent electrodes *Int. J. Extrem. Manuf.* **5** 015503

[7] Zhang H, Sun F, Feng J, Ling H, Zhou D, Cao G, Wang S, Su F, Tian Y and Tian Y 2022 A stable, self-regulating, flexible, ITO-free electrochromic smart window for energy-efficient buildings *Cell Rep. Phys. Sci.* **3** 101193

[8] Choi S *et al* 2015 Stretchable heater using ligand-exchanged silver nanowire nanocomposite for wearable articular thermotherapy *ACS Nano* **9** 6626–33

[9] Shin K-Y, Hong J-Y, Lee S and Jang J 2012 High electrothermal performance of expanded graphite nanoplatelet-based patch heater *J. Mater. Chem.* **22** 23404–10

[10] Bagherifard S, Tamayol A, Mostafalu P, Akbari M, Comotto M, Annabi N, Ghaderi M, Sonkusale S, Dokmeci M R and Khademhosseini A 2016 Dermal patch with integrated flexible heater for on demand drug delivery *Adv. Healthcare Mater.* **5** 175–84

[11] Gong M, Wan P, Ma D, Zhong M, Liao M, Ye J, Shi R and Zhang L 2019 Flexible breathable nanomesh electronic devices for on-demand therapy *Adv. Funct. Mater.* **29** 1902127

[12] Liu Q, Tian B, Liang J and Wu W 2021 Recent advances in printed flexible heaters for portable and wearable thermal management *Mater. Horiz.* **8** 1634–56

[13] Kim T, Kim Y W, Lee H S, Kim H, Yang W S and Suh K S 2013 Uniformly interconnected silver-nanowire networks for transparent film heaters *Adv. Funct. Mater.* **23** 1250–5

[14] Ahn J, Gu J, Hwang B, Kang H, Hwang S, Jeon S, Jeong J and Park I 2019 Printed fabric heater based on Ag nanowire/carbon nanotube composites *Nanotechnology* **30** 455707

[15] Huang Q and Zhu Y 2019 Printing conductive nanomaterials for flexible and stretchable electronics: a review of materials, processes, and applications *Adv. Mater. Technol.* **4** 1800546

[16] Byers K M, Lin L-K, Moehling T J, Stanciu L and Linnes J C 2020 Versatile printed microheaters to enable low-power thermal control in paper diagnostics *Analyst* **145** 184–96

[17] Mitra D, Grummt A, Thalheim R and Zichner R 2023 Reliability and potential of inkjet-printed flexible heaters with adaptive temperature zones for high-temperature and long-time applications *Energy Technol.* **11** 2200874

[18] Hu X, Wang S, Zhang H, Wang Y, Hang C, Wen J and Tian Y 2021 Silver flake/polyaniline composite ink for electrohydrodynamic printing of flexible heaters *J. Mater. Sci., Mater. Electron.* **32** 27373–83

[19] Wang P-H, Chen S-P, Su C-H and Liao Y-C 2015 Direct printed silver nanowire thin film patterns for flexible transparent heaters with temperature gradients *RSC Adv.* **5** 98412–8

[20] Huang Q, Al-Milaji K N and Zhao H 2018 Inkjet printing of silver nanowires for stretchable heaters *ACS Appl. Nano Mater.* **1** 4528–36

[21] Huang D, Taha M S, Nocera A L, Workman A D, Amiji M M and Bleier B S 2023 Cold exposure impairs extracellular vesicle swarm–mediated nasal antiviral immunity *J. Allergy Clin. Immunol.* **151** 509–25